Burns & Trauma, 2024, 12, tkad025
https://doi.org/10.1093/burnst/tkad025
Research Article

OXFORD

Research Article

Matrix metalloproteinase-8 regulates dendritic cell tolerance in late polymicrobial sepsis via the nuclear factor kappa-B p65/β-catenin pathway

Zhong-qiu Lu[1], Chen Zhang[1], Lin-jun Zhao[1,2], Wei Dong[1], Liang Lv[1], Yang Lu[3], Xiao-Yan Chen[1], Jie Zhang[1], Xin-yong Liu[1], Zhong Xiao[1], Long-wang Chen[1], Yong-ming Yao[4,*] and Guang-ju Zhao[1,*]

[1]Department of Emergency Medicine, The First Affiliated Hospital of Wenzhou Medical University, Fanhai West Road, Ouhai District, Wenzhou 325000, China, [2]Translational Medicine Research Center, Medical Innovation Research Division and Fourth Medical of the Chinese PLA General Hospital, Fucheng Road, Haidian District, Beijing 100048, China, [3]Department of Emergency Medicine, Affiliated Hangzhou First People's Hospital, Zhejiang University School of Medicine, Huansha Road,Shangcheng District, Hangzhou 310006, China and [4]Department of Rheumatology, Wenzhou People's Hospital, Gu'an road, Ouhai district, Wenzhou 325000, China

*Correspondence.Guang-ju Zhao, Email: zgj_0523@126.com; Yong-ming Yao, Email: c_ff@sina.com

Received 19 November 2022; Revised 24 March 2023; Editorial decision 17 April 2023

Abstract

Background: Tolerogenic dendritic cells (DCs) are associated with poor prognosis of sepsis. Matrix metalloproteinases (MMPs) have been shown to have immunomodulatory effects. However, whether MMPs are involved in the functional reprogramming of DCs is unknown. The study aims to investigate the role of MMPs in sepsis-induced DCs tolerance and the potential mechanisms.

Methods: A murine model of late sepsis was induced by cecal ligation and puncture (CLP). The expression levels of members of the MMP family were detected in sepsis-induced tolerogenic DCs by using microarray assessment. The potential roles and mechanisms underlying MMP8 in the differentiation, maturation and functional reprogramming of DCs during late sepsis were assessed both *in vitro* and *in vivo*.

Results: DCs from late septic mice expressed higher levels of MMP8, MMP9, MMP14, MMP19, MMP25 and MMP27, and MMP8 levels were the highest. MMP8 deficiency significantly alleviated sepsis-induced immune tolerance of DCs both *in vivo* and *in vitro*. Adoptive transfer of MMP8 knockdown post-septic bone marrow-derived DCs protected mice against sepsis-associated lethality and organ dysfunction, inhibited regulatory T-cell expansion and enhanced Th1 response. Furthermore, the effect of MMP8 on DC tolerance was found to be associated with the nuclear factor kappa-B p65/β-catenin pathway.

Conclusions: Increased MMP8 levels in septic DCs might serve as a negative feedback loop, thereby suppressing the proinflammatory response and inducing DC tolerance.

Graphical Abstract

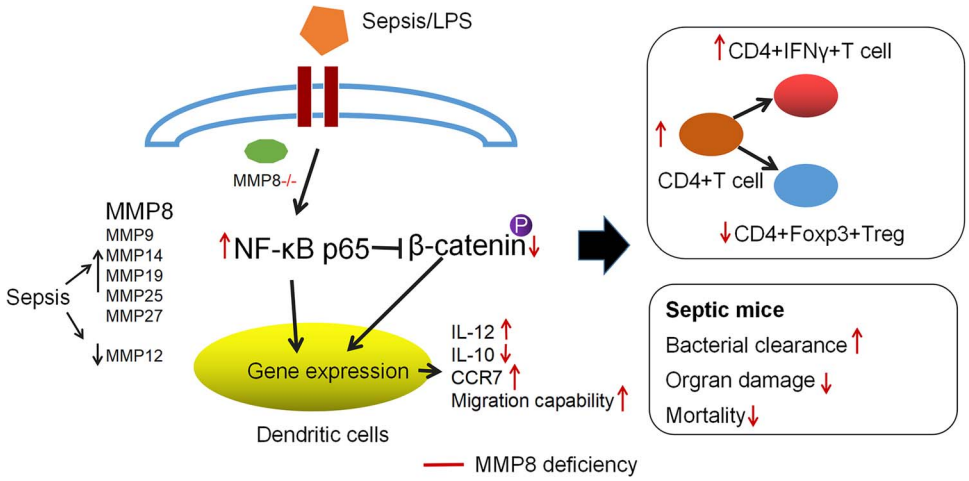

Key words: Sepsis, Dendritic cells, Immune tolerance, Matrix metalloproteinases, Signaling pathway, β-catenin, Nuclear factor kappa-B

Highlights

- DCs from late septic mice expressed higher levels of MMP8, MMP9, MMP14, MMP19, MMP25 and MMP27, and MMP8 was the highest.
- MMP8 deficiency significantly alleviated sepsis-induced immune tolerance of DCs both *in vivo* and *in vitro*.
- Adoptive transfer of MMP8 knockdown post-septic BMDCs protected mice against sepsis-associated lethality and organ dysfunction, inhibited regulatory T cell expansion and enhanced Th1 response.
- The effect of MMP8 on DC tolerance in sepsis was associated with the nuclear factor kappa-B p65/β-catenin pathway.

Background

The innate immune response is the first line of host defense against invading pathogens. During infection and sepsis, innate immune cells are activated and induce an adaptive immune response to kill invading microorganisms. Studies by our group and others have demonstrated a sustained reduction in dendritic cells (DCs) in lymphoid organs in the setting of sepsis and infection [1–3]. In addition, in response to microbial components, DCs from hosts with polymicrobial sepsis exhibit maturation defects, have an impaired ability to produce interleukin (IL)-12 and secrete high levels of IL-10 [4, 5]. This functional reprogramming of DCs may contribute to immunoparalysis and poor prognosis in patients with infection [6, 7].

Upon infection, to detect pathogens and initiate defense responses, DCs are equipped with various cell surface receptors. Pathogen-derived molecules, such as lipopolysaccharide (LPS), bind with toll-like receptor (TLR) 4 to induce the activation of nuclear factor kappa-B (NF-κB) signaling, leading to DC maturation and activation [8, 9]. Conversely, the activation of β-catenin signaling is usually responsible for programming DCs to tolerant states and downregulating the inflammatory response [10]. Interestingly, studies on NF-κB have shown that it plays a crucial role in regulating β-catenin signaling during inflammation and infection [11, 12]. NF-κB activation represses the β-catenin pathway by inhibiting its nuclear translocation, which indicates the potential role of the NF-κB/β-catenin pathway in regulating DC function.

Matrix metalloproteinases (MMPs) are a family of zinc-dependent endopeptidases that has >20 members [13]. MMPs are well known for their important roles in degradation and remodeling of the extracellular matrix [14]. Previous reports have shown that extracellular MMPs may exert cell signaling by cleaving secreted proteins as well as surface receptors and ligands [15–17]. However, in addition to extracellular effects, studies have found that MMPs are expressed intracellularly in cardiomyocytes, endothelial cells, neurons and immune cells [13, 18, 19]. A heightened proinflammatory phenotype has been noted in MMP14-null macrophages, and increased levels of MMP9 after LPS stimulation contribute to TLR4 activation in leukocytes [18, 19]. Whether MMPs are involved in the functional reprogramming of DCs, however, is largely unknown.

Notably, although MMPs are expressed across most tissues, some of them are only expressed by specific cell types [20]. Strikingly, different MMPs may have different functions in immune responses, as mentioned above. In the present study, after evaluating the phenotype and function of DCs in a mouse septic peritonitis model, the expression characteristics of MMP family members in DCs during late sepsis were determined by using microarray analysis. Furthermore, we

focused on MMP8, which had the highest expression level among 23 MMPs in DCs during late sepsis. The potential roles and mechanisms underlying the role of MMP8 in the differentiation, maturation and functional reprogramming of DCs during peritonitis-induced polymicrobial sepsis were assessed both *in vitro* and *in vivo*.

Methods

Animals

Mice deficient in MMP-8 ($MMP8^{-/-}$) (C57BL/6 background, aged 6–8 weeks) were obtained from GemPharmatech Co., Ltd, Jiangsu, China. Wild-type C57BL/6 mice (aged 6–8 weeks) were purchased from GemPharmatech Co., Ltd, Jiangsu, China and Beijing Vital River Laboratory Animal Technology Co., Ltd, Beijing, China.

Septic peritonitis model induced by cecal ligation and puncture

A septic mouse model was established by cecal ligation and puncture (CLP) [21, 22]. C57BL/6 mice were anesthetized with chloral hydrate and fixed in the supine position. The abdominal skin was disinfected and a midline abdominal incision was made. The cecum was exposed, ligated and perforated with a 21- or 25-gauge needle. After extruding the intestinal contents, the cecum was placed back into the abdominal cavity. Then, abdominal incisions were sutured. Sham-operated mice underwent laparotomy to expose the cecum, but the cecum was not ligated and punctured. Both septic mice and sham mice received 1 ml of sterile isotonic saline injection.

Cell preparation

The spleen was removed from mice aseptically and placed in phosphate buffer solution (PBS). After trituration and passing through a mesh, splenocytes were harvested. To obtain mononuclear cells, splenocytes were further purified by Ficoll-Paque density gradient centrifugation. CD11c is commonly used as a marker for dendritic cells, and CD11c MicroBeads have been widely used by us and other researchers to isolate DCs and explore their functions [1,23–25]. So, in the present study, mouse CD11c MicroBeads were used to isolate DCs from mononuclear cells by a positive selection method (Miltenyi Biotech, Bergisch Gladbach, Germany). DCs derived from bone marrow (BMDCs) were also prepared to further confirm the functional changes in DCs [26]. In brief, BM cells from septic mice or sham mice were cultured with 20 ng/ml murine recombinant granulocyte-macrophage colony-stimulating factor (GM-CSF) (PeproTech, USA) for 7 days. Additionally, $CD11c^{+}$BMDCs were purified with CD11c MicroBeads (Miltenyi Biotech, Bergisch Gladbach, Germany) for adoptive transfer experiments and for testing cell-migration capabilities (Figure S1).

Microarray analysis

For Affymetrix microarray profiling, total RNA was isolated from splenic DCs with TRIzol reagent (Karlsbad Invitrogen, Canada), treated with DNase and then purified with an RNeasy Mini Kit (Qiagen, Hilden, Germany). The quantity and quality of RNA were measured with a UV–Vis spectrophotometer (Thermo, nanodrop 2000, USA) at an absorbance of 260 nm. The mRNA expression profile was detected by GeneChip Mouse Transcriptome Array 1.0 (Affymetrix GeneChip, Santa Clara, CA, USA). Affymetrix Expression Console Software (Version 1.2.1) was used for microarray analysis. To normalize the raw data (CEL files) at the transcript level, robust multiarray average normalization was performed, and then the expression value of each transcript was calculated. The gene-level data were then screened to include only those probe sets that appeared in the 'core' meta-probe list representing the RefSeq gene.

Two-hit model

DCs from septic mice were treated with 1000 ng/ml LPS from *Escherichia coli* (Sigma, USA) as a 'second hit'. To establish a two-hit model *in vivo*, septic mice on day 3 post-CLP were treated with LPS at a dose of 2 mg/kg via a single intraperitoneal injection.

Flow cytometric analysis

To test the levels of $CD11c^{+}$ cells and conventional DCs, the cells were incubated with anti-mouse CD11c-fluorescein isothiocyanate (FITC) antibody and/or major histocompatibility complex class II (MHC-II)-Allophycocyanin (APC) antibody (eBioscience, San Diego, CA, USA) or isotype control antibodies for 30 min on ice. Additionally, after surface staining of CD4 using a CD4-FITC antibody (BD Biosciences, San Diego, CA, USA), cells were fixed and permeabilized using Cytofix/Cytoperm (BD Biosciences) and then incubated with anti-mouse interferon (IFN)-γ or forkhead box P3 (Foxp3) antibodies (BD Biosciences, San Diego, CA, USA). Flow cytometry analysis was performed with a BD FACSCanto II flow cytometer (BD Biosciences, San Diego, CA, USA).

Cell transfection and stimulation

MMP8 small interfering RNA (siRNA) was used to knock down the expression of MMP8 in BMDCs or $CD11c^{+}$BMDCs. MMP8 siRNA and its control siRNA used in the present study were obtained from Santa Cruz Biotechnology (Santa Cruz, CA, USA). In brief, at 7 days from the initial culture, the total BMDCs and $CD11c^{+}$BMDCs were harvested. The cells were seeded in a 6-well plate with 2.5×10^{6} cells per well supplemented with 2.5 ml of culture medium. Six hours later, 0.5 ml of culture medium containing 60 pmol MMP8/control siRNA and 7.5 μl of Lipofectamine 3000 reagent (Invitrogen, Allen Way Carlsbad, CA, USA)

were added to each well. After 24 h of incubation, the culture medium was replaced with new medium. Another 24 h later, the cells were harvested for further experiments. The transfection efficiency was detected by western blot analysis. For maturation and activation experiments, at 24 h of transfection, the cells were treated with LPS (1000 ng/ml) (Sigma–Aldrich, St Louis, MO, USA) for 24 h. The cells were occasionally treated with JSH-23 (Selleck, USA), an NF-κB inhibitor, for 24 h after MMP8 siRNA transfection.

Adoptive transfer

A total of 2×10^6 CD11c$^+$BMDCs were injected intraperitoneally into septic mice at 6 h after CLP. The mice were sacrificed 24 h after injection, immediately followed by the harvesting of lung, kidney, spleen and blood.

Western blotting

Cells were washed with 1 × PBS and lysed in RIPA lysis buffer (Solarbio, Beijing, China). In some experiments, lysis buffer containing protease inhibitors (Solarbio, Beijing, China) was used. A nuclear and cytoplasmic protein extraction kit (Beyotime, China) was used to extract nuclear and cytoplasmic proteins from the cells. Cell lysates were separated by sodium dodecyl sulfate-polyacrylamide gel electrophoresis (SDS-PAGE) and transferred to polyvinylidene fluoride (PVDF) membranes. Then, the membranes were probed with the indicated antibodies. Histone H3, NF-κB p65, phospho-β-catenin and β-catenin antibodies were obtained from Cell Signaling Technology (Cell Signaling, USA). Beta-tubulin antibody was purchased from Proteintech (USA). MMP8 and glyceraldehyde-3-phosphate dehydrogenase (GAPDH) antibodies were obtained from Abcam (Abcam, Cambridge, UK).

Polymerase chain reaction

Total RNA was extracted from DCs using TRIzol reagent (Invitrogen, Carlsbad, CA, USA). After reverse transcription, cDNAs were amplified by using SYBR green PCR master mix (Thermo Fisher Scientific) using a thermal cycler (Applied Biosystems, Foster City, CA, USA). The primers used in the present study are shown in Table S1, see online supplementary material.

Enzyme-linked immunosorbent assay

The levels of IL-12p70 and IL-10 in plasma and cell culture supernatant were detected by commercial enzyme-linked immunosorbent assay (ELISA) kits provided by Multi Sciences (Multi Sciences, Hangzhou, China).

Migration assay

CD11c$^+$BMDCs (5×10^5) were added to the upper chamber of a transwell in serum-free medium. RPMI 1640 medium containing 20% fetal bovine serum and 20 ng/ml mouse recombinant chemokine (C-C motif) ligand 21 (CCL21) (PeproTech, USA) was added to the lower chamber. The number of CD11c$^+$ cells in the lower chamber was counted by flow cytometry.

Histological examination

Lung and kidney tissue samples were fixed in 10% formalin and then placed in fresh formalin for 24 h. After paraffin embedding, the lung and kidney samples were cut into sections (5 μm) and stained with hematoxylin and eosin (HE). Images were observed and captured using an Olympus BX40F microscope (Olympus, Melville, NY, USA).

Immunofluorescence

To perform immunofluorescence tests, DCs were grown on cell culture chamber slides. After washing with PBS three times, DCs were fixed with 4% paraformaldehyde and permeabilized with 0.3% Triton X-100 (Solarbio, Beijing, China) for 30 min at 37°C. After washing, 1% BSA (Solarbio, Beijing, China) was used to block the cells. Subsequently, slides were incubated with anti-mouse β-catenin or NF-κB p65 primary antibodies at 4°C overnight. Then, after washing with PBS, slides were probed with different fluorescent secondary antibodies (Abcam, Cambridge, UK) for 1 h at room temperature. The nuclei were incubated with 10 μl of DAPI solution (Solarbio, Beijing, China). The localization of β-catenin or NF-κB p65 was then detected by fluorescence microscopy (Leica, Germany).

Statistical analysis

Statistical analyses were performed using the GraphPad 8.0 statistical program (GraphPad software, San Diego, CA, USA) and SPSS statistical software (IBM SPSS Statistics 22.0). Our data were normally distributed and are presented as the mean ± standard deviation (SD). Differences between two groups were assessed using Student's t test. One-wayAnalysis of Variance (ANOVA) followed by least significant difference *post hoc* analysis was used to compare the differences among multiple groups. The survival rate was analyzed by Kaplan–Meier analysis and compared by the log-rank test, and Fisher's exact test was used to compare the survival rate between groups at certain time points. $P < 0.05$ was accepted as a statistically significant difference.

Results

Phenotype and function of splenic DCs and BMDCs in late sepsis

A mouse model with moderate severe sepsis was induced by CLP. Approximately 40–60% of the septic mice died within the first 48 h post-CLP, but not thereafter (Figure 1a). Therefore, with reference to the results of our previous animal and clinical research [26–29], the phenotype and function of DCs were evaluated on day 3 post-CLP. As shown in Figure 1b–d, the number of mononuclear cells and CD11c$^+$ cells and the percentage of CD11c$^+$ cells among mononuclear

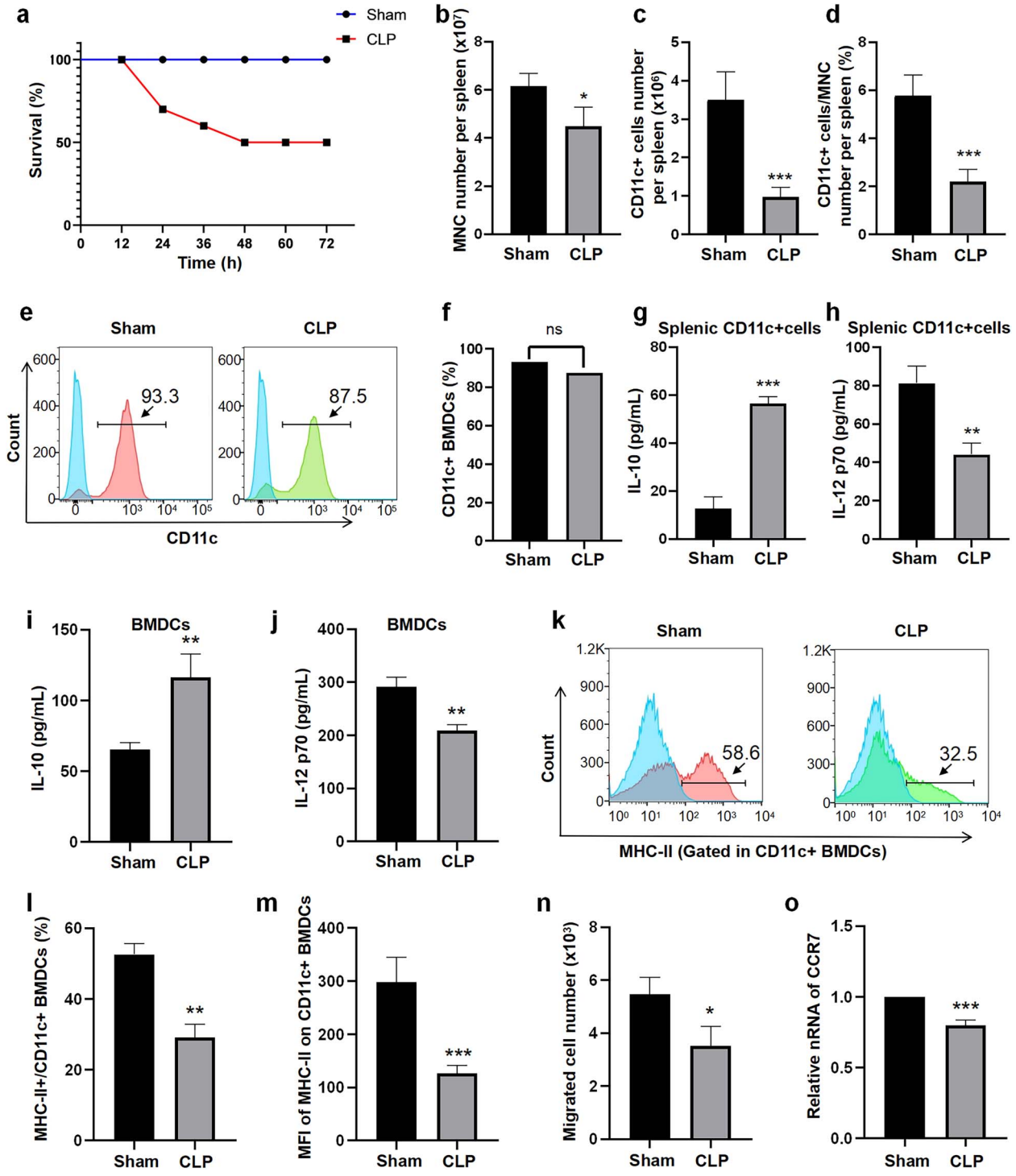

Figure 1. Phenotype and function of splenic and bone marrow (BM)-derived dendritic cells (DCs) in septic mice. (**a**) Mortality in the different experimental groups (10 mice/group) was recorded every 12 h. (**b**, **c**) The absolute numbers of mononuclear cells (MNCs) and CD11c-positive cells per spleen. (**d**) The percentages of CD11c-positive cells in MNCs per spleen. (**e**, **f**) Representative flow cytometric analysis was performed to determine the percentages of CD11c-positive cells in BM-derived cells. Cytokine production (IL-10 and IL-12p70) by splenic CD11c-positive cells (**g**, **h**) and BMDCs (**i**, **j**) was measured following 24 h of treatment with LPS. (**k**, **l**) Representative flow cytometric analysis was performed to determine the percentages of $MHCII^{+}$ cells among BMDCs. (**m**) The median fluorescence intensity (MFI) of MHC-II on BMDCs. (**n**) The number of migrated BM-derived CD11c-positive cells was determined by flow cytometry. (**o**) The mRNA levels of CCR7 were tested by RT-PCR. Data are shown as the mean ± SD (n = 3); $^{***}p < 0.001$, $^{**}p < 0.01$ and $^{*}p < 0.05$; ns, not significant. *CLP* cecal ligation and puncture, *BMDCs* bone marrow derived dendritic cells, *CCR7* chemokine C-C-motif receptor 7, *MHC* major histocompatibility complex class, *RT-PCR* reverse transcription-polymerase chain reaction

cells were significantly deceased in spleens from septic mice on day 3 post-CLP compared with sham mice. As shown in Figure 1e, f, compared to that from sham mice, the activity of BM cells from septic mice to generate CD11c-positive DCs decreased slightly, and there was no statistical significance.

After treatment with LPS for 24 h, the production of IL-12p70, a key host defense cytokine, was decreased in supernatants of splenic $CD11c^+$ cells and BMDCs from septic mice compared with sham mice on day 3 post-CLP, while IL-10 levels were significantly increased (Figure 1 g–j). The percentage of MHC-II-positive cells ($MHC\text{-}II^+$) among CD11c-positive BMDCs and the median fluorescence intensity (MFI) of CD11c-positive BMDCs from septic mice were lower than those of cells from sham mice (Figure 1k–m). Additionally, the migration capability of post-septic BM-derived CD11c-positive DCs was lower than that of cells from sham mice (Figure 1n). As chemokine C-C-motif receptor 7 (CCR7) is necessary to direct DCs to secondary lymphoid nodes, the expression of CCR7 was also assessed, and the results showed that the DCs generated from the BM of CLP mice expressed lower levels of CCR7 (Figure 1o).

Expression patterns of MMPs in tolerogenic dendritic cells during late sepsis

Splenic DCs were isolated from septic and sham mice. A total of 23 members of the MMP family were detected in sepsis-induced tolerogenic DCs by using microarray assessment. Among them, DCs from the spleens of septic mice on day 3 post-CLP expressed higher levels of MMP8, MMP9, MMP14, MMP19, MMP25 and MMP27 than DCs from the spleens of sham mice, and MMP8 levels were the highest, with a 25-fold increase (Figure 2a, b). The levels of MMP12 in splenic DCs from septic mice were lower than those in splenic DCs from sham mice, while there were no significant differences in the levels of MMP1a/b, MMP2, MMP3, MMP7, MMP10, MMP11, MMP13, MMP15, MMP16, MMP17, MMP20, MMP21, MMP23, MMP24 and MMP28 in splenic DCs between septic and sham mice (Figure 2a and b).

The mRNA levels of MMP8 in post-septic splenic $CD11c^+$ cells and BMDCs were confirmed by reverse transcription-PCR (RT-PCR). As shown in Figure 2c, d, both post-septic splenic $CD11c^+$ cells and BMDCs expressed higher levels of MMP8 mRNA than cells from sham mice. Because most MMPs are secretory proteins, the protein levels of MMP8 in DCs were further determined by western blotting analysis. The results showed that the levels of MMP8 protein in post-septic splenic $CD11c^+$ cells were significantly higher than those in sham cells (Figure 2e g). Similar results were observed in DCs generated from BM cells (Figure 2f, h).

Genetic inhibition of MMP8 of sepsis-induced immune tolerance of DCs *in vitro*

To investigate the potential role of MMP8 in the sepsis-induced immune tolerance of DCs, BMDCs from septic mice were transfected with MMP8 siRNA. MMP8 knockdown cells exhibited significantly decreased expression of MMP8 compared to the cells in the CLP group and the control siRNA group (Figure 3a–c). Our results showed that MMP8 knockdown had no effect on the percentage of $CD11c^+MHC\text{-}II^+$ cells in BMDCs and slightly increased the MFI of MHC-II of CD11c-positive cells (Figure 3d–f).

As shown in Figure 3g, IL-12p70 levels were significantly elevated in MMP8 siRNA-transfected cells in response to LPS stimulation. In contrast, the protein levels of IL-10 were lower in post-septic BMDCs than in BMDCs from sham mice. MMP8 knockdown BMDCs exhibited significantly lower levels of IL-10 than post-septic BMDCs (Figure 3h). As shown in Figure 3i, MMP8 knockdown significantly augmented the migration capability of post-septic CD11c-positive BMDCs. In addition, the mRNA levels of CCR7 in the cells were enhanced after MMP8 siRNA transfection (Figure 3j).

MMP8 deficiency alleviates sepsis-induced immune tolerance of DCs *in vivo*

To investigate whether MMP8 plays a role in sepsis-induced immune tolerance of DCs *in vivo*, wild-type and $MMP8^{-/-}$ septic mice were stimulated with LPS as a 'second hit' on day 3 post-CLP. $MMP8^{-/-}$ septic mice had a higher percentage of $CD11c^+$ cells in the spleen in response to LPS than wild-type septic mice (Figure 4a). The percentage of $MHC\text{-}II^+$ cells in $CD11c^+$ cells was also higher in $MMP8^{-/-}$ septic mice than in wild-type septic mice (Figure 4b). $MMP8^{-/-}$ septic mice had higher levels of IL-12p70 and lower levels of IL-10 in the plasma (Figure 4c, d, respectively).

As shown in Figure 3e, after treatment with LPS for 12 h, there was a significant difference in the percentage of CD4-positive cells among the splenic mononuclear cells of wild-type and $MMP8^{-/-}$ septic mice (Figure 4e). Additionally, $MMP8^{-/-}$ septic mice had a lower percentage of $CD4^+Foxp3^+$ regulatory T cells (Tregs) and a higher percentage of $CD4^+IFN\text{-}\gamma^+T$ cells in the spleen than wild-type septic mice (Figure 4f, g).

Adoptive transfer of post-septic DCs transfected with MMP8 siRNA protects mice from fatal sepsis

As shown in Figure 4, CD11c-positive BMDCs from sham or post-septic mice transfected with MMP8 siRNA were intraperitoneally injected into CLP mice. The bacterial load in the lung and peripheral blood at 24 h after CLP was determined. CLP mice that had received MMP8 knockdown CLP-BMDCs contained a lower bacterial load in the lung and peripheral blood (Figure 5a, b, and Figure S2a, see online supplementary material). MMP8 knockdown CLP-BMDC treatment significantly reduced the lung and kidney tissue pathological scores in mice secondary to sepsis (Figure 5c, d and Figure S2b) Treatment with a single injection of MMP8 knockdown CLP-BMDCs from septic mice but not CLP-BMDCs transfected with control siRNA protected mice against CLP-induced fatal outcomes at 24 h (Figure 5e, f).

As shown in Figure 5, treatment with sham BMDCs, but not CLP BMDCs, significantly reduced the percentage of $CD4^+Foxp3^+$Treg cells in the spleens of septic mice.

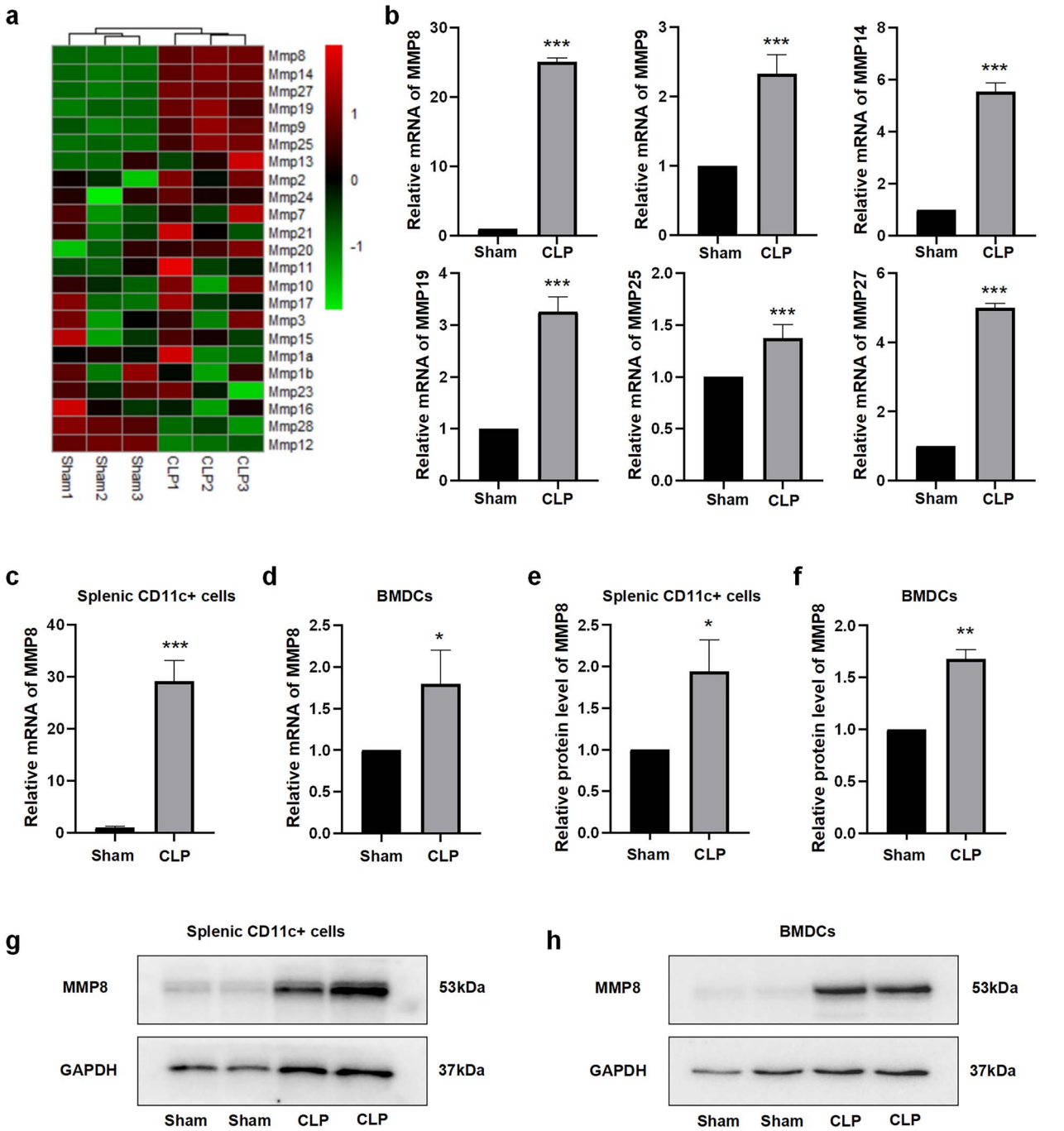

Figure 2. Expression patterns of MMPs in tolerogenic DCs during late sepsis. (**a**) Heatmaps depicting the expression levels of MMPs in splenic DCs from septic and sham mice. (**b**) Histogram depicting the levels of MMPs that increased in splenic DCs 3 days post-CLP. The mRNA levels of MMP8 in splenic CD11c-positive cells (**c**) and BMDCs (**d**). Representative immunoblots and densitometric values of MMP8 in splenic CD11c-positive cells (**e**, **g**) and BMDCs (**f**, **h**) are shown; β-actin was used as the loading control. n = 3, $^{***}p < 0.001$, $^{**}p < 0.01$ and $^{*}p < 0.05$. *CLP* cecal ligation and puncture, *MMP* matrix metalloproteinase, *BMDCs* bone marrow-derived dendritic cell, *MHC* major histocompatibility complex class

Moreover, the MMP8 knockdown CLP-BMDC group had lower percentages of $CD4^+Foxp3^+$Treg cells and higher levels of $CD4^+IFN\text{-}\gamma^+$T cells in the spleen than the CLP-BMDC group (Figure 5g–i, and Figure S3 see online supplementary material). Septic mice treated with MMP8 knockdown CLP-BMDCs had a higher level of IL-12p70 and a lower level of IL-10 in the plasma than mice treated with CLP-BMDCs (Figure 5j, k, respectively).

MMP8 knockdown enhances NF-kB p65 nuclear translocation and suppresses β-catenin activity in DCs

NF-κB is well known to perform critical roles in DC maturation and cytokine production as well as migration [30]. As indicated in Figure 5a, the nuclear and cytoplasmic protein levels of NF-κB p65 in CD11c-positive BMDCs in response to LPS were tested by western blotting. We found that nuclear protein NF-κB p65 expression in

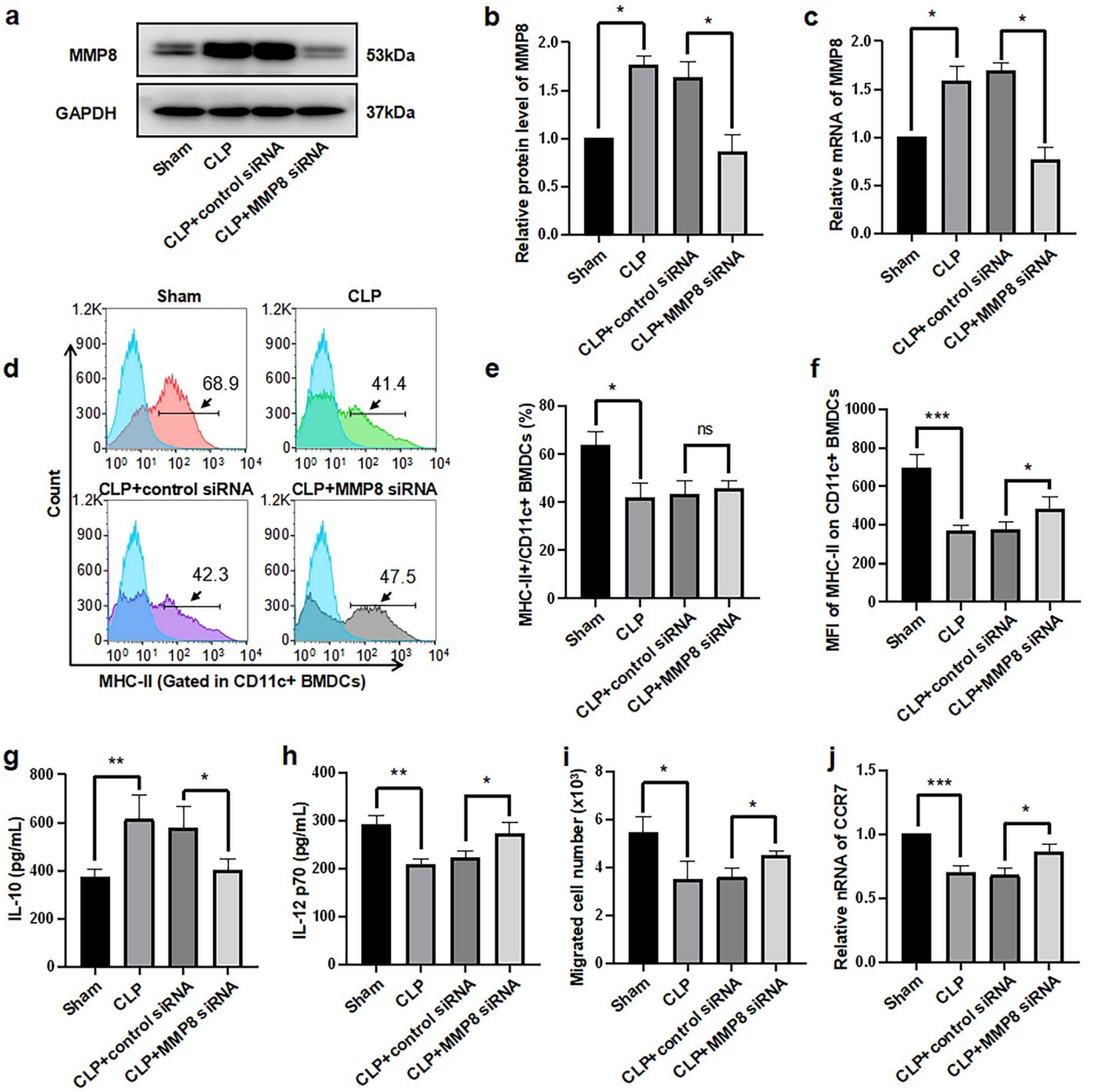

Figure 3. MMP8 knockdown on sepsis-induced immune tolerance of DCs *in vitro*. (**a, b**) Western blot analysis was used to determine the expression levels of MMP8 in BMDCs. (**c**) The mRNA levels of MMP8 in BMDCs were determined by RT-PCR. (**d, e**) Representative flow cytometric analysis was performed to determine the percentage of $MHCII^+$ cells among CD11c-positive BMDCs. (**f**) The median fluorescence intensity (MFI) of MHC-II on CD11c-positive BMDCs. IL-10 (**g**) and IL-12p70 (**h**) levels in the supernatants of BMDCs were detected by ELISA. (**i**) The number of migrated CD11c-positive BMDCs was measured by flow cytometry. (**j**) mRNA levels of CCR7 were determined by RT-PCR. Data are shown as the mean ± SD (n = 3); $^{***}p < 0.001$, $^{**}p < 0.01$ and $^{*}p < 0.05$. *CLP* cecal ligation and puncture, *MMP8* matrix metalloproteinase 8, *BMDCs* bone marrow-derived dendritic cell, *MHC* major histocompatibility complex class, *siRNA* small interfering RNA, *CCR7* chemokine C-C-motif receptor 7

CLP-BMDCs was lower than that in BMDCs from sham mice after LPS stimulation. MMP8 knockdown significantly upregulated the protein levels of NF-κB p65 in the nucleus (Figure 6a, b). The nuclear translocation of NF-κB p65 in DCs was further determined by fluorescence microscopy. We noted that the nuclear translocation of NF-kB p65 in CLP-BMDCs following LPS treatment was lower than that in BMDCs from sham mice. MMP8 knockdown promoted the nuclear translocation of NF-kB p65 in CLP-BMDCs (Figure 6c).

Recent studies on β-catenin have documented that it is crucial in inducing immune tolerance in DCs [10, 31, 32]. As shown in Figure 6, the phosphorylation levels of β-catenin at Ser552 in BMDCs in response to LPS were tested. The results revealed that there was a greater proportion of β-catenin phosphorylated at Ser552 in CLP-BMDCs than in cells from

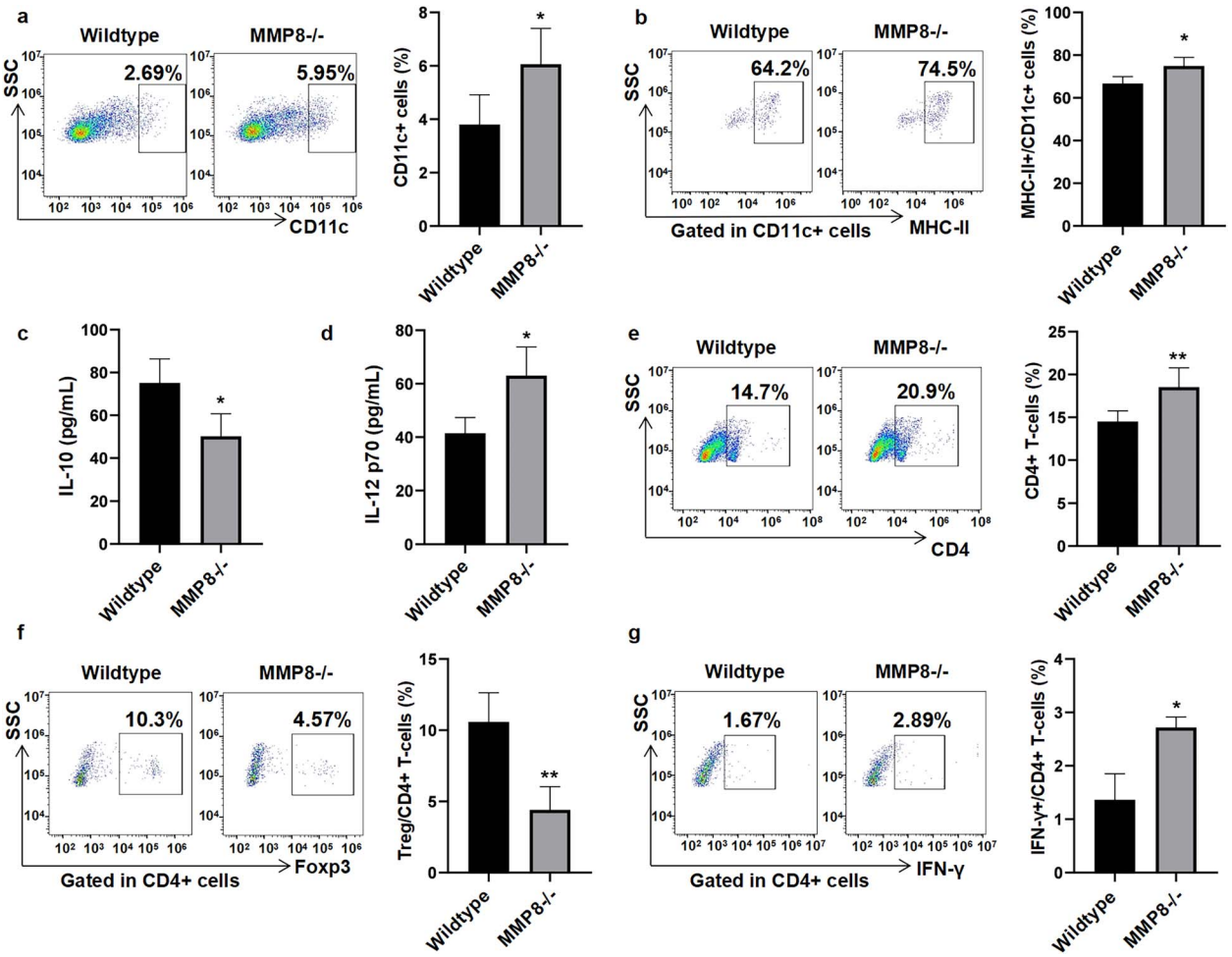

Figure 4. MMP8 deficiency alleviates sepsis-induced immune tolerance of DCs and Treg expansion in a 'two-hit' mouse model. The percentages of $CD11c^+$ (**a**) and $CD11c^+MHCII^+$ (**b**) cells in the spleen were determined by flow cytometric analysis. The protein levels of IL-10 (**c**) and IL-12p70 (**d**) in the plasma were tested by ELISA. Flow cytometric analysis was used to assess the percentages of $CD4^+$ (**e**), $CD4^+Foxp3^+$ (**f**) and $CD4^+IFN\text{-}\gamma^+$ (**g**) T cells in the spleen. n = 6, $^{**}p < 0.01$ and $^{*}p < 0.05$. *CLP* cecal ligation and puncture, *MMP8* matrix metalloproteinase 8, *IL* interleukin, *IFN* interferon, *Foxp3* forkhead box P3, *MHC* major histocompatibility complex class

sham mice. MMP8 knockdown CLP-BMDCs had a lower proportion of phosphorylated β-catenin at Ser552 than CLP-BMDCs (Figure 6d, e). Following LPS challenge, we found that sepsis *per se* resulted in augmented nuclear translocation of β-catenin in BMDCs that was inhibited by MMP8 gene knockdown. The results indicated that upregulation of MMP8 may be responsible for sepsis-induced inactivation of NF-κB p65 and activation of β-catenin in BMDCs (Figure 6f).

Inhibition of NF-kB suppresses the function of DCs and promotes β-catenin activation in response to LPS after MMP8 knockdown

The results showed that the expression levels of nuclear NF-κB p65 were significantly downregulated after treatment with JSH-23, an NF-κB inhibitor, in MMP8 knockdown CLP-BMDCs (Figure 7a, b). As shown in Figure 7c, d, the protein levels of IL-12p70 were lower and the levels of IL-10 were higher in CLP-BMDCs than in MMP8 knockdown CLP-BMDCs. JSH-23 treatment significantly reversed the elevation in IL-12p70 levels and the reduction in IL-10 levels after MMP8 knockdown (Figure 7c, d, respectively). The migration capability of post-septic CLP-BMDCs and the expression of CCR7 after MMP8 knockdown were suppressed by inhibiting NF-κB activation (Figure 7e, f).

A previous study demonstrated that NF-κB can repress the activation of β-catenin [12]. In the current study, the activation of β-catenin after inhibiting NF-κB in MMP8 knockdown CLP-BMDCs was also assessed. As shown in Figure 7g–i, the levels of phosphorylated β-catenin Ser552 as well as its nuclear translocation were decreased in CLP-BMDCs after MMP8 knockdown. However, JSH-23 treatment reversed the activation of β-catenin in MMP8 knockdown cells. Our results illustrate that the effect of MMP8 on DCs may be achieved via, at least in part, the NF-κB p65/β-catenin pathway.

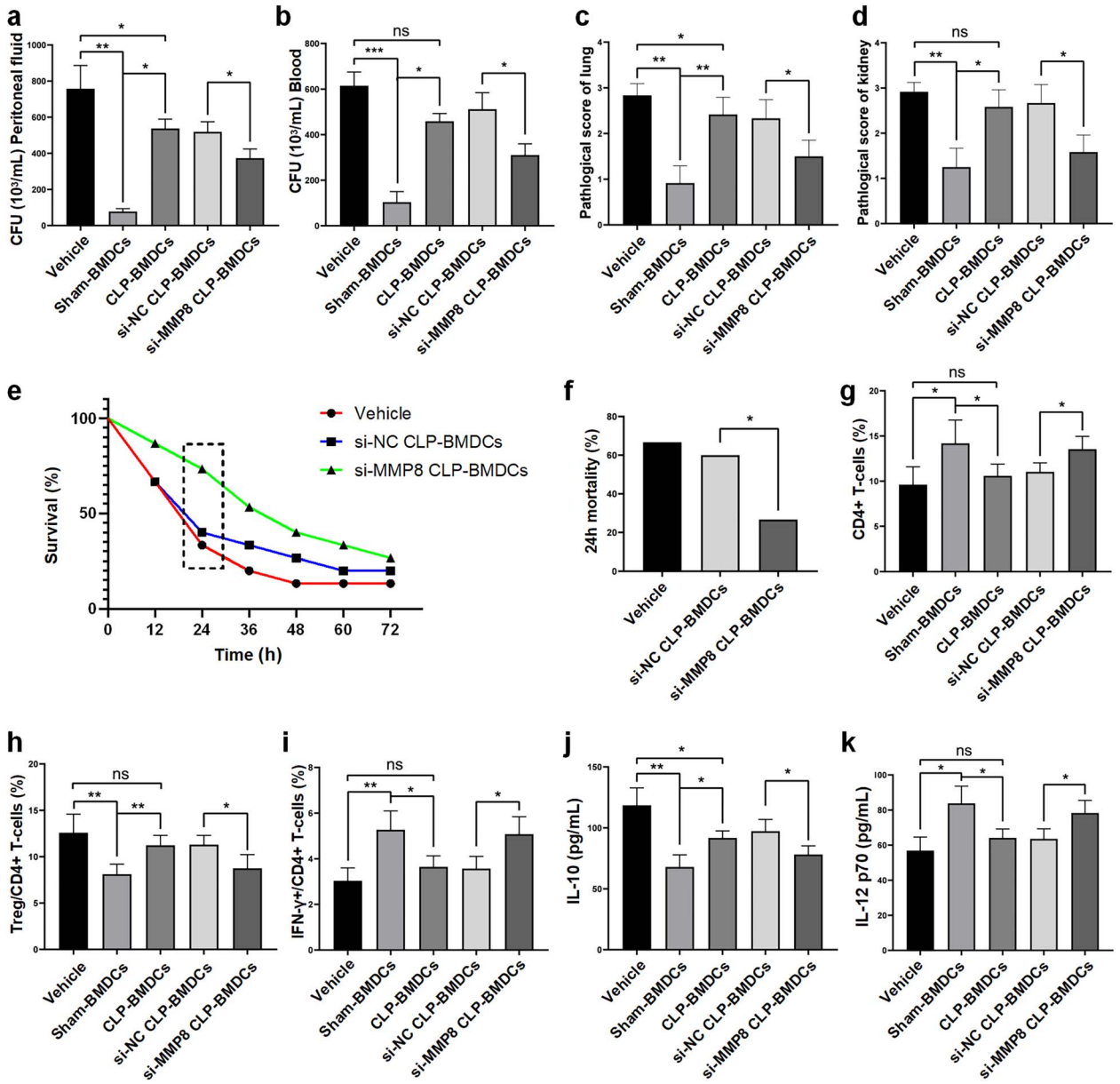

Figure 5. Adoptive transfer of post-septic BMDCs transfected with MMP8 siRNA protects mice from fatal outcomes. Peritoneal fluid (**a**) and peripheral blood (**b**) at 24 h after CLP were collected for culturing. The number of bacterial colonies was counted (n = 3). Pathological score of lung (**c**) and renal tissues (**d**) in each group (n = 6). (**e**) Mortality in the different groups (15 mice/group) was recorded every 12 h. (**f**) Mortality differences between the groups were compared at the 24-h time point after surgery. Flow cytometric analysis was performed to determine the percentages of $CD4^+$ (**g**), $CD4^+Foxp3^+$ (**h**) and $CD4^+IFN\text{-}\gamma^+$ (**i**) T cells in the spleen. The levels of IL-10 (**j**) and IL-12p70 (**k**) in the plasma were measured by ELISA. Data are expressed as the mean ± SD (n = 5); $^{**}p < 0.01$ and $^{*}p < 0.05$; ns, not significant. *CLP* cecal ligation and puncture, *BMDCs* bone marrow-derived dendritic cells, *MMP8* matrix metalloproteinase 8, *si-NC* negative control small interfering RNA (siRNA), *si-MMP8* MMP8 small interfering RNA (siRNA), *MMP8 m*atrix metalloproteinase 8, *Treg* regulatory T cell, *IL* interleukin, *IFN-*γ interferon-γ, *ELISA* enzyme-linked immunosorbent assay

Discussion

We have demonstrated for the first time that MMP8 programs DCs to a tolerogenic state in polymicrobial sepsis. DCs are classified as critical antigen-presenting cells that play important roles in recognizing pathogens and regulating the immune response and inflammation. Similar to the results of previous studies [5, 33], a profound loss of $CD11c^+$ cells from the spleen during sepsis was also evident in the present study. Interestingly, the ability of BMCs from septic mice to generate $CD11c^+$ cells was comparable to that of cells from sham mice. We also noticed that both splenic $CD11c^+$ and BM-derived DCs in sepsis were impaired in acquiring a mature state in response to LPS. These paralyzed DCs secreted more IL-10 but failed to express IL-12p70. Migration to peripheral lymph organs is required for DCs to prime naive T lymphocytes and has been shown to involve CCR7-mediated signaling [34].

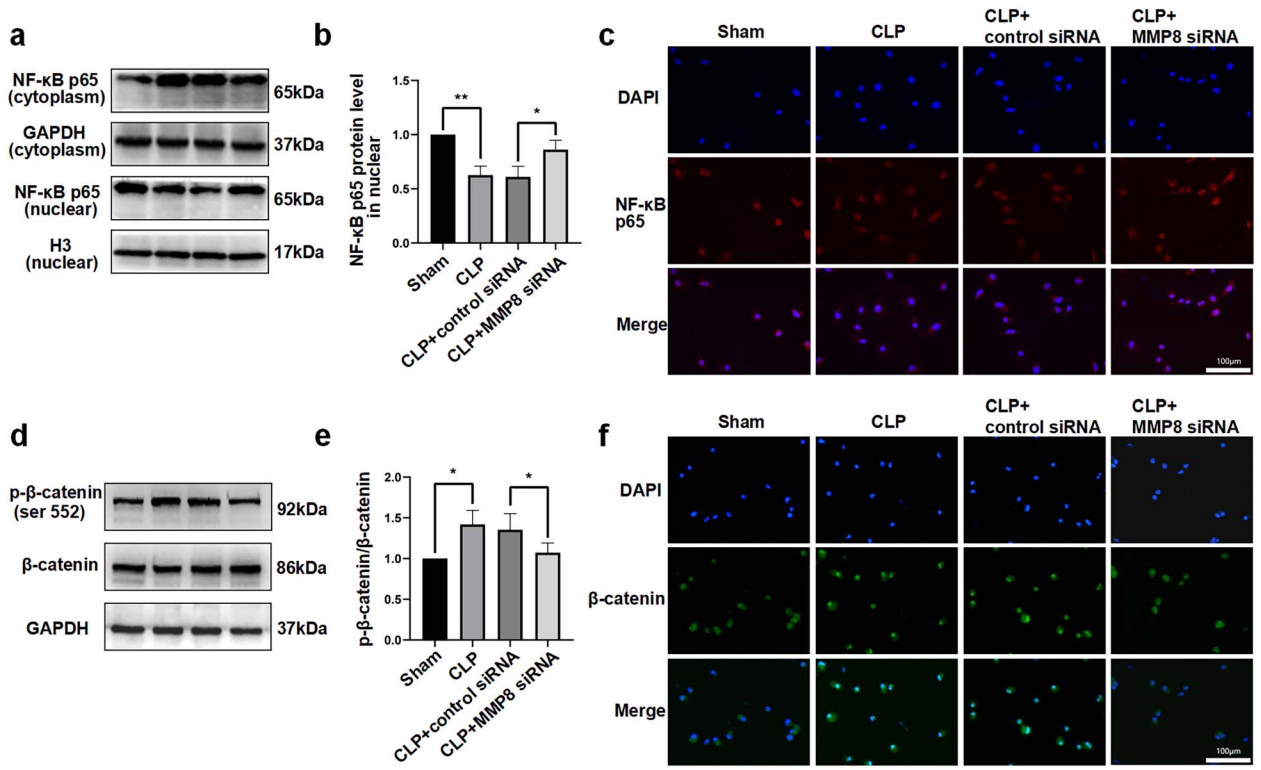

Figure 6. MMP8 knockdown enhances NF-kB p65 nuclear translocation and suppresses β-catenin activity in BMDCs. Western blotting was used to detect the nuclear and cytoplasmic protein levels of NF-κB p65 (**a**) and phospho-β-catenin (**d**) in BMDCs. The relative nuclear protein levels of NF-κB p65 (**b**) and ratios of β-catenin to total β-catenin (**e**) are shown (n = 4 or 5). Nuclear translocation of p65 (**c**) and β-catenin (**f**) was analyzed by immunofluorescence (n = 3). Scale bar: 100 μm. Data are shown as the mean ± SD; $^{**}p < 0.01$ and $^{*}p < 0.05$. *CLP* cecal ligation and puncture, *MMP8* matrix metalloproteinase 8, *siRNA* small interfering RNA, *NF-κB* nuclear factor kappa-B, *GAPDH* glyceraldehyde-3-phosphate dehydrogenase, *H3* histone 3

Thus, the impaired migration capability of DCs and decreased expression levels of CCR7 may contribute to the dysfunction of the immune response upon septic challenge.

In the current study, we found that the expression of MMP8 appeared to be significantly increased in septic DCs. MMP8, also known as neutrophil collagenase and collagenase 2, is a secreted protease that degrades extracellular matrix proteins during inflammatory tissue destruction [35]. Similar to other MMPs, extracellular MMP8 regulates the immune response by cleaving chemokines as well as other signaling factors [35, 36]. Recently, research interest in MMPs has shifted to their biological functions in signal transduction [37, 38]. For example, MMP12 is required for interferon secretion and the subsequent antiviral immune response [39]. Interestingly, in the present study, the expression of MMP12 was decreased in septic DCs, which might partly explain the higher levels of viral replication in patients with sepsis [40]. It has been reported that the mRNA and protein levels of MMP8 in blood from sepsis patients are significantly higher than those of controls [41, 42]. Additionally, a study showed that MMP8 knockout juvenile mice are more susceptible to infection [42]. Interestingly, genetic ablation or pharmacologic inhibition of MMP8 decreases acute inflammation in adult mice at 6 h after sepsis [43]. Nevertheless, the levels of MMP8 in DCs and its immunomodulatory effect in late sepsis have not been clarified. Herein, using a late sepsis model and MMP8 knockout mice, we found that MMP8 deficiency significantly alleviated sepsis-induced immune tolerance of DCs both *in vivo* and *in vitro*. Moreover, adoptive transfer of MMP8 knockdown post-septic BMDCs, but not post-septic BMDCs, protected mice from polymicrobial sepsis-induced death, organ dysfunction and Treg expansion. These findings indicate that the role of MMP8 in sepsis may be influenced by developmental age as well as the stage of sepsis.

The decreased activity of NF-κB, a core inducer of proinflammatory cytokines, is one of the important characteristics of tolerogenic DCs [44]. There are five members of the NF-κB family, including p50, p52, Rel, Rel-A (p65) and Rel-B [45, 46]. Upon cytokine or LPS stimulation, NF-κB p65 forms dimers with other NF-κB subunits, mainly p50, and then translocates into the nucleus, where it mediates the activation of target genes, including IL-12p70 and CCR7 [46, 47]. NF-κB p65 might be involved in MMP8-mediated functional reprogramming of DCs because nuclear translocation in septic DCs was obviously enhanced after MMP8 knockdown, and the elevated levels of IL-12p70 and CCR7 in septic DCs after MMP8 knockdown were reversed by treatment with an NF-κB inhibitor.

In addition to NF-κB, we noted that β-catenin signaling, another conserved pathway, might also play a role in inducing

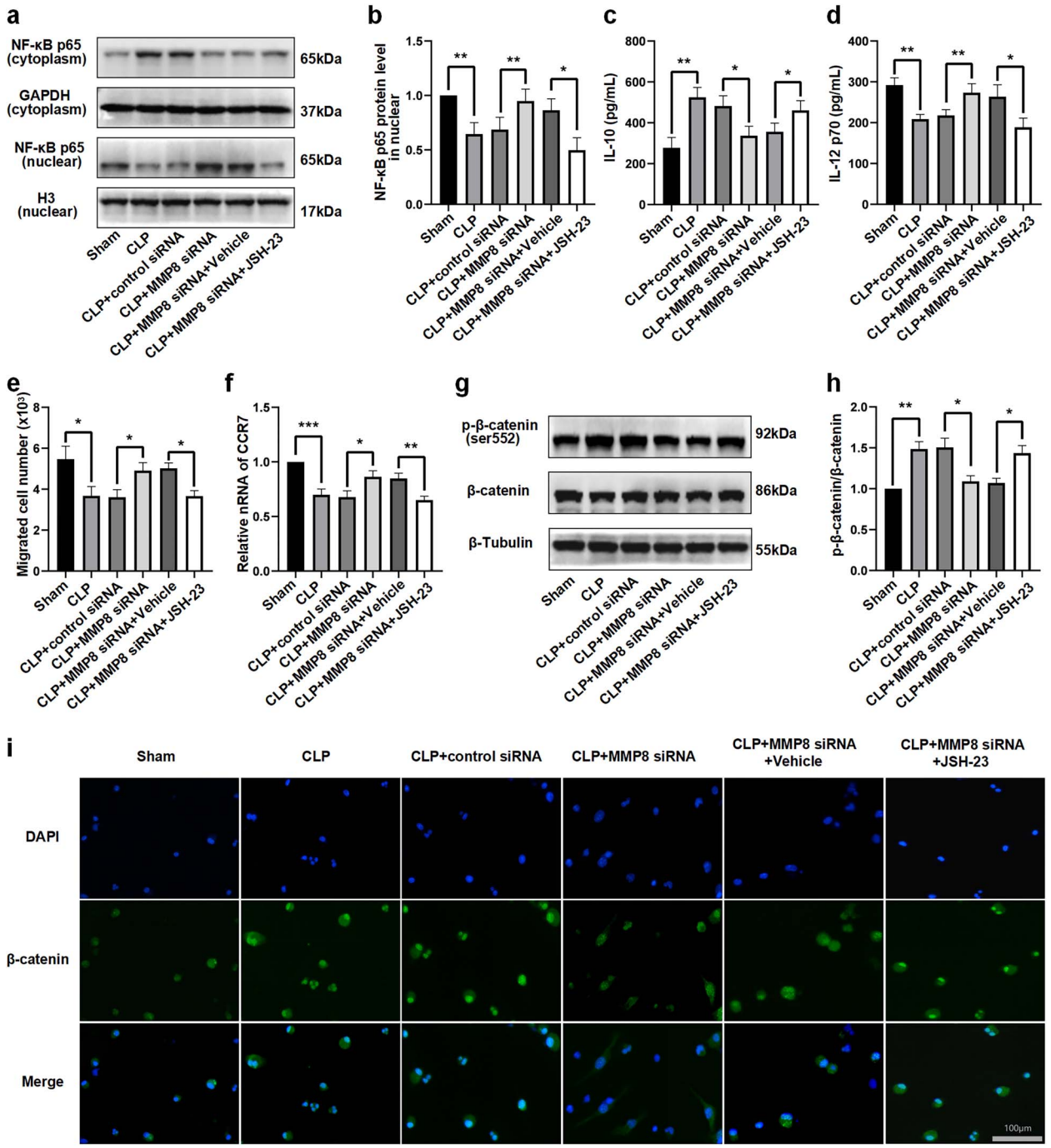

Figure 7. Inhibition of NF-kB suppresses the function of DCs and promotes β-catenin activation in response to LPS after MMP8 knockdown. (**a**, **b**) Western blotting was used to determine nuclear and cytoplasmic protein levels of p65. ELISA was performed to test the levels of IL-10 (**c**) and IL-12p70 (**d**) secreted by CD11c + BMDCs. (**e**) The number of migrated CD11c-positive BMDCs was assessed by flow cytometry. (**f**) mRNA levels of CCR7 were determined by RT–PCR. (**g**, **h**) The protein levels of phospho-β-catenin were measured by western blotting. (**i**) Nuclear translocation of β-catenin analyzed by immunofluorescence. Scale bar: 100 μm. Data are shown as the mean ± SD, n = 3; *** $p < 0.001$, ** $p < 0.01$ and * $p < 0.05$. *CLP* cecal ligation and puncture, *MMP8* matrix metalloproteinase 8, *siRNA* small interfering RNA, *NF-κB* nuclear factor kappa-B, *GAPDH* glyceraldehyde-3-phosphate dehydrogenase, *H3* histone 3, *IL* interleukin, *CCR7* chemokine C-C-motif receptor 7, *LPS* lipopolysaccharide

tolerance in DCs in sepsis. Previous studies have shown that in intestinal DCs and E-cadherin-stimulated DCs, β-catenin is required for the expression of anti-inflammatory mediators, including IL-10 and transforming growth factor-β, and subsequent Treg expansion [10, 48]. Interestingly, some studies have reported that NF-κB can negatively regulate the activity of the β-catenin pathway through direct and indirect mechanisms. In colon, liver and breast cancer cells, p65 overexpression indirectly regulates the nuclear translocation of β-catenin by inducing leucine zipper tumor suppressor 2

(lzts2) expression [49]. The p65/p50 dimer as well as the activators of the NF-κB pathway have been shown to directly interact with β-catenin and then regulate β-catenin-dependent transcriptional activity [50, 51]. In the present study, inhibition of NF-kB promoted the activation of β-catenin and inhibited the immune response of DCs after MMP8 knockout. We believe that the NF-kB/β-catenin pathway contributes to MMP8-mediated DC tolerance. However, in addition to its role in dampening inflammation, previous studies have reported that β-catenin was associated with enhanced inflammatory cytokine production in splenic DCs, indicating the complex roles of β-catenin in regulating the function of DCs [52, 53].

Conclusion

The present study identified the expression patterns of MMP family members in tolerogenic dendritic cells and the role of MMP8 in sepsis-induced dendritic cell tolerance and immune dysfunction. The effect of MMP8 on DC tolerance was associated with the NF-κB p65/β-catenin pathway. Further studies may be needed to investigate the other mechanisms involved in MMP8-mediated functional reprogramming of immune cells and their clinical significance.

Abbreviations

BMDC: Bone marrow derived dendritic cell; CCR: Chemokine C-C-motif receptor; CLP: Cecal ligation and puncture; DC: Dendritic cells; ELISA: Enzyme-linked immunosorbent assay; Foxp3: Forkhead box P3; GAPDH: Glyceraldehyde-3-phosphate dehydrogenase; H3: Histone 3; IFN: Interferon; IL: Interleukin; LPS: Lipopolysaccharide; MFI: Median fluorescence intensity; MHC: Major histocompatibility complex class; MMPs: Matrix metalloproteinases; NF-κB: Nuclear factor kappa-B; RT-PCR: Reverse transcription-polymerase chain reaction; siRNA: Small interfering RNA.

Supplementary data

Supplementary data is available at *Burns & Trauma Journal* online.

Funding

This work was supported partly by grants from the National Natural Science Foundation of China (81871583), Key R&D Program Projects of Zhejiang Province (2021C03072), and the Natural Science Foundation of Zhejiang Province (LQ19H100003).

Data availability

The datasets generated and/or analyzed during the current study are available from the corresponding author on reasonable request.

Authors' contributions

ZQL conceptualized and drafted the manuscript. CZ, LJZ, WD and LL performed the major experiments. YL, XYC, JZ, XYL, ZX and LWC collected the data and contributed to flow cytometric analysis. GJZ and YMY designed the experiments and supervised and revised the manuscript.

Ethics approval

All animal experiments were carried out according to the Guides for the Care and Use of Laboratory Animals, National Academy of Sciences, China. The present animal study was approved by the Laboratory Animal Ethics Committee of Wenzhou Medical University (SYXK-2017-0033).

Conflicts of interest

None declared.

References

1. Wang LX, Ren C, Yao RQ, Luo YN, Yin Y, Wu Y, *et al*. Sestrin2 protects against lethal sepsis by suppressing the pyroptosis of dendritic cells. *Cell Mol Life Sci*. 2021;78:8209–27.
2. Zhang Y, Chen L, Luo Y, Wang K, Liu X, Xiao Z, *et al*. Pink1/parkin-mediated Mitophagy regulated the apoptosis of dendritic cells in sepsis. *Inflammation*. 2022;45:1374–87.
3. Delano MJ, Ward PA. Sepsis-induced immune dysfunction: can immune therapies reduce mortality? *J Clin Invest*. 2016;126:23–31.
4. Bouras M, Asehnoune K, Roquilly A. Contribution of dendritic cell responses to sepsis-induced immunosuppression and to susceptibility to secondary pneumonia. *Front Immunol*. 2018;9:2590.
5. Venet F, Demaret J, Gossez M, Monneret G. Myeloid cells in sepsis-acquired immunodeficiency. *Ann N Y Acad Sci*. 2021;1499:3–17.
6. Poehlmann H, Schefold JC, Zuckermann-Becker H, Volk HD, Meisel C. Phenotype changes and impaired function of dendritic cell subsets in patients with sepsis: a prospective observational analysis. *Crit Care*. 2009;13:R119.
7. Du K, Hao S, Luan H. Expression of peripheral blood DCs CD86, CD80, and Th1/Th2 in sepsis patients and their value on survival prediction. *Comput Math Methods Med*. 2022;2022:4672535.
8. Ghislat G, Cheema AS, Baudoin E, Verthuy C, Ballester PJ, Crozat K, *et al*. NF-κB-dependent IRF1 activation programs cDC1 dendritic cells to drive antitumor immunity. *Sci Immunol*. 2021;6:eabg3570.
9. Mulas F, Wang X, Song S, Nishanth G, Yi W, Brunn A, *et al*. The deubiquitinase OTUB1 augments NF-κB-dependent immune responses in dendritic cells in infection and inflammation by stabilizing UBC13. *Cell Mol Immunol*. 2021;18:1512–27.
10. Manicassamy S, Reizis B, Ravindran R, Nakaya H, Salazar-Gonzalez RM, Wang YC, *et al*. Activation of beta-catenin in dendritic cells regulates immunity versus tolerance in the intestine. *Science*. 2010;329:849–53.
11. Nejak-Bowen K, Kikuchi A, Monga SP. Beta-catenin-NF-κB interactions in murine hepatocytes: a complex to die for. *Hepatology*. 2013;57:763–74.
12. Hwang I, Choi YS, Jeon MY, Jeong S. NF-κB p65 represses β-catenin-activated transcription of cyclin D1. *Biochem Biophys Res Commun*. 2010;403:79–84.

13. Bassiouni W, Ali M, a M, Schulz R. Multifunctional intracellular matrix metalloproteinases: implications in disease. *FEBS J*. 2021;288:7162–82.
14. Cabral-Pacheco GA, Garza-Veloz I, Castruita-De La Rosa C, Ramirez-Acuña JM, Perez-Romero BA, Guerrero-Rodriguez JF, *et al*. The roles of matrix Metalloproteinases and their inhibitors in human diseases. *Int J Mol Sci*. 2020;21:9739.
15. De Bock M, Wang N, Decrock E, Bultynck G, Leybaert L. Intracellular cleavage of the Cx43 C-terminal domain by matrix-metalloproteases: a novel contributor to inflammation? *Mediat Inflamm*. 2015;2015:257471.
16. Dean RA, Cox JH, Bellac CL, Doucet A, Starr AE, Overall CM. Macrophage-specific metalloelastase (MMP-12) truncates and inactivates ELR+ CXC chemokines and generates CCL2, −7, −8, and −13 antagonists: potential role of the macrophage in terminating polymorphonuclear leukocyte influx. *Blood*. 2008;112:3455–64.
17. Aota K, Ono S, Yamanoi T, Kani K, Momota Y, Azuma M. MMP-9 inhibition suppresses interferon-γ-induced CXCL10 production in human salivary gland ductal cells. *Inflammation*. 2019;42:2148–58.
18. Klose A, Zigrino P, Mauch C. Monocyte/macrophage MMP-14 modulates cell infiltration and T-cell attraction in contact dermatitis but not in murine wound healing. *Am J Pathol*. 2013;182:755–64.
19. Zhang Z, Amorosa LF, Coyle SM, Macor MA, Lubitz SE, Carson JL, *et al*. Proteolytic cleavage of AMPKα and intracellular MMP9 expression are both required for TLR4-mediated mTORC1 activation and HIF-1α expression in leukocytes. *J Immunol*. 2015;195:2452–60.
20. Nissinen L, Kähäri VM. Matrix metalloproteinases in inflammation. *Biochim Biophys Acta*. 2014;1840:2571–80.
21. Hu ZQ, Yao YM, Chen W, Bian JL, Zhao LJ, Chen LW, *et al*. Partial depletion of regulatory T cells enhances host inflammatory response against acute Pseudomonas aeruginosa infection after sepsis. *Inflammation*. 2018;41:1780–90.
22. Yao RQ, Li ZX, Wang LX, Li YX, Zheng LY, Dong N, *et al*. Single-cell transcriptome profiling of the immune space-time landscape reveals dendritic cell regulatory program in polymicrobial sepsis. *Theranostics*. 2022;12:4606–28.
23. Vogel A, Martin K, Soukup K, Halfmann A, Kerndl M, Brunner JS, *et al*. JAK1 signaling in dendritic cells promotes peripheral tolerance in autoimmunity through PD-L1-mediated regulatory T cell induction. *Cell Rep*. 2022;38:110420.
24. Zamora-Pineda J, Kumar A, Suh JH, Zhang M, Saba JD. Dendritic cell sphingosine-1-phosphate lyase regulates thymic egress. *J Exp Med*. 2016;213:2773–91.
25. Li JY, Ren C, Wang LX, Yao RQ, Dong N, Wu Y, *et al*. Sestrin2 protects dendrite cells against ferroptosis induced by sepsis. *Cell Death Dis*. 2021;12:834.
26. Guak H, Al Habyan S, Ma EH, Aldossary H, Al-Masri M, Won SY, *et al*. Glycolytic metabolism is essential for CCR7 oligomerization and dendritic cell migration. *Nat Commun*. 2018;9:2463.
27. Chen W, Lian J, Ye JJ, Mo QF, Qin J, Hong GL, *et al*. Ethyl pyruvate reverses development of Pseudomonas aeruginosa pneumonia during sepsis-induced immunosuppression. *Int Immunopharmacol*. 2017;52:61–9.
28. Zhao GJ, Li D, Zhao Q, Song JX, Chen XR, Hong GL, *et al*. Incidence, risk factors and impact on outcomes of secondary infection in patients with septic shock: an 8-year retrospective study. *Sci Rep*. 2016;6:38361.
29. Wang Z, Li Z, Ji H. Direct targeting of β-catenin in the Wnt signaling pathway: current progress and perspectives. *Med Res Rev*. 2021;41:2109–29.
30. Van Delft MA, Huitema LF, Tas SW. The contribution of NF-κB signalling to immune regulation and tolerance. *Eur J Clin Investig*. 2015;45:529–39.
31. Karnam A, Bonam SR, Rambabu N, Wong SSW, Aimanianda V, Bayry J. Wnt-β-catenin Signaling in human dendritic cells mediates regulatory T-cell responses to fungi via the PD-L1 pathway. *MBio*. 2021;12:e0282421.
32. Valenta T, Hausmann G, Basler K. The many faces and functions of β-catenin. *EMBO J*. 2012;31:2714–36.
33. Efron PA, Martins A, Minnich D, Tinsley K, Ungaro R, Bahjat FR, *et al*. Characterization of the systemic loss of dendritic cells in murine lymph nodes during polymicrobial sepsis. *J Immunol*. 2004;173:3035–43.
34. Liu J, Zhang X, Cheng Y, Cao X. Dendritic cell migration in inflammation and immunity. *Cell Mol Immunol*. 2021;18:2461–71.
35. Juurikka K, Butler GS, Salo T, Nyberg P, Åström P. The role of MMP8 in cancer: a systematic review. *Int J Mol Sci*. 2019;20:4506.
36. Van Lint P, Libert C. Matrix metalloproteinase-8: cleavage can be decisive. *Cytokine Growth Factor Rev*. 2006;17:217–23.
37. Figiel I, Kruk PK, Zaręba-Kozioł M, Rybak P, Bijata M, Wlodarczyk J, *et al*. MMP-9 Signaling pathways that engage rho GTPases in brain plasticity. *Cell*. 2021;10:166.
38. Guan C, Xiao Y, Li K, Wang T, Liang Y, Liao G. MMP-12 regulates proliferation of mouse macrophages via the ERK/P38 MAPK pathways during inflammation. *Exp Cell Res*. 2019;378:182–90.
39. Marchant DJ, Bellac CL, Moraes TJ, Wadsworth SJ, Dufour A, Butler GS, *et al*. A new transcriptional role for matrix metalloproteinase-12 in antiviral immunity. *Nat Med*. 2014;20:493–502.
40. Walton AH, Muenzer JT, Rasche D, Boomer JS, Sato B, Brownstein BH, *et al*. Reactivation of multiple viruses in patients with sepsis. *PLoS One*. 2014;9:e98819.
41. Wong HR, Cvijanovich N, Allen GL, Lin R, Anas N, Meyer K, *et al*. Genomic expression profiling across the pediatric systemic inflammatory response syndrome, sepsis, and septic shock spectrum. *Crit Care Med*. 2009;37:1558–66.
42. Solan PD, Dunsmore KE, Denenberg AG, Odoms K, Zingarelli B, Wong HR. A novel role for matrix metalloproteinase-8 in sepsis. *Crit Care Med*. 2012;40:379–87.
43. Atkinson SJ, Varisco BM, Sandquist M, Daly MN, Klingbeil L, Kuethe JW, *et al*. Matrix Metalloproteinase-8 augments bacterial clearance in a juvenile sepsis model. *Mol Med*. 2016;22:455–63.
44. Carreño LJ, Riedel CA, Kalergis AM. Induction of tolerogenic dendritic cells by NF-κB blockade and Fcγ receptor modulation. *Methods Mol Biol*. 2011;677:339–53.
45. Smale ST. Dimer-specific regulatory mechanisms within the NF-κB family of transcription factors. *Immunol Rev*. 2012;246:193–204.
46. Yu Y, Feng S, Wei S, Zhong Y, Yi G, Chen H, *et al*. Extracellular ATP activates P2X7R-NF-κB (p65) pathway to promote the maturation of bone marrow-derived dendritic cells of mice. *Cytokine*. 2019;119:175–81.

47. Yu N, Wang S, Song X, Gao L, Li W, Yu H, *et al*. Low-dose radiation promotes dendritic cell migration and IL-12 production via the ATM/NF-KappaB pathway. *Radiat Res*. 2018;189:409–17.
48. Fu C, Jiang A. Generation of tolerogenic dendritic cells via the E-cadherin/beta-catenin-signaling pathway. *Immunol Res*. 2010;46:72–8.
49. Cho HH, Song JS, Yu JM, Yu SS, Choi SJ, Kim DH, *et al*. Differential effect of NF-kappaB activity on beta-catenin/Tcf pathway in various cancer cells. *FEBS Lett*. 2008;582:616–22.
50. Lamberti C, Lin KM, Yamamoto Y, Verma U, Verma IM, Byers S, *et al*. Regulation of beta-catenin function by the IkappaB kinases. *J Biol Chem*. 2001;276:42276–86.
51. Schwitalla S, Fingerle AA, Cammareri P, Nebelsiek T, Göktuna SI, Ziegler PK, *et al*. Intestinal tumorigenesis initiated by dedifferentiation and acquisition of stem-cell-like properties. *Cell*. 2013;152:25–38.
52. Zirnheld AL, Villard M, Harrison AM, Kosiewicz MM, Alard P. β-Catenin stabilization in NOD dendritic cells increases IL-12 production and subsequent induction of IFN-γ-producing T cells. *J Leukoc Biol*. 2019;106:1349–58.
53. Cohen SB, Smith NL, Mcdougal C, Pepper M, Shah S, Yap GS, *et al*. Beta-catenin signaling drives differentiation and proinflammatory function of IRF8-dependent dendritic cells. *J Immunol*. 2015;194:210–22.